AD-A108 548 NAVAL RESEARCH LAB WASHINGTON DC F/G 11/6
COMPARISON OF NOTCH-STRESS WITH STRAIN-CONTROLLED LOW CYCLE FAT--ETC(U)
DEC 81 J M KRAFFT, G R YODER
UNCLASSIFIED NRL-MR-4697 NL

END
DATE FILMED
1 82
DTIC

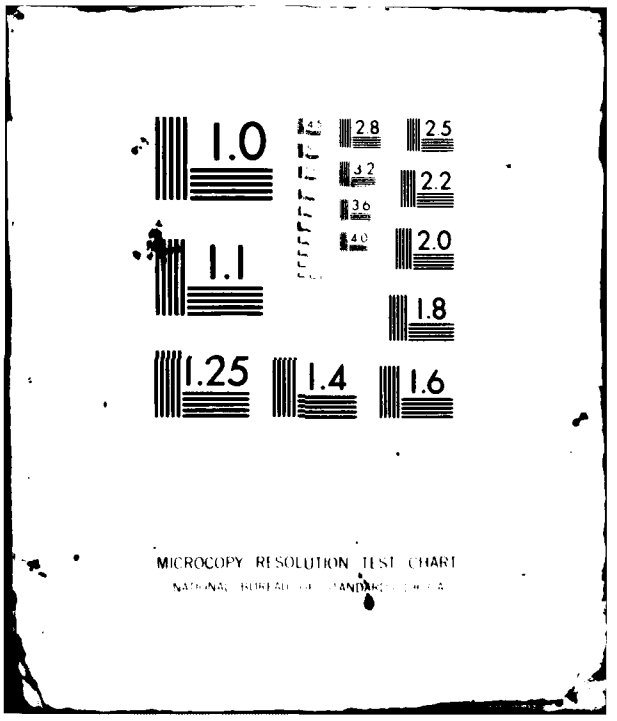
1.0
1.1
1.25
1.4
1.6
1.8
2.0
2.2
2.5
2.8
3.2
3.6
4.0
MICROCOPY RESOLUTION TEST CHART

SECURITY CLASSIFICATION OF THIS PAGE (When Data Entered)

REPORT DOCUMENTATION PAGE	READ INSTRUCTIONS BEFORE COMPLETING FORM
1. REPORT NUMBER: NRL Memorandum Report 4697	2. GOVT ACCESSION NO.: AD-A105548
3. RECIPIENT'S CATALOG NUMBER	
4. TITLE (and Subtitle): COMPARISON OF NOTCH-STRESS WITH STRAIN-CONTROLLED LOW CYCLE FATIGUE OF ALPHA-BETA TITANIUM ALLOYS	5. TYPE OF REPORT & PERIOD COVERED: Interim report on a continuing NRL problem.
	6. PERFORMING ORG. REPORT NUMBER
7. AUTHOR(s): J.M. Krafft and G.R. Yoder	8. CONTRACT OR GRANT NUMBER(s)
9. PERFORMING ORGANIZATION NAME AND ADDRESS: Naval Research Laboratory, Washington, DC 20375	10. PROGRAM ELEMENT, PROJECT, TASK AREA & WORK UNIT NUMBERS: 58-0264; WR-22-01-01; 63-1054; WR-22-01-01
11. CONTROLLING OFFICE NAME AND ADDRESS	12. REPORT DATE: December 4, 1981
	13. NUMBER OF PAGES: 12
14. MONITORING AGENCY NAME & ADDRESS(if different from Controlling Office)	15. SECURITY CLASS. (of this report): UNCLASSIFIED
	15a. DECLASSIFICATION/DOWNGRADING SCHEDULE

16. DISTRIBUTION STATEMENT (of this Report)

Approved for public release; distribution unlimited.

17. DISTRIBUTION STATEMENT (of the abstract entered in Block 20, if different from Report)

18. SUPPLEMENTARY NOTES

19. KEY WORDS (Continue on reverse side if necessary and identify by block number)

Low cycle fatigue
Crack initiation
Titanium alloys
Notch stress fatigue

20. ABSTRACT (Continue on reverse side if necessary and identify by block number)

Prior studies of present authors provided two different tests of low cycle fatigue endurance of the same set of titanium alloys. Strain controlled push-pull deformation of axial specimens covered crack initiation life of up to 10^3 cycles. Notch stress controlled tensile load cycling extended the range to 10^6 cycles. All of Ti-6Al-4V, the test materials varied in oxygen content and in effective grain size. The results could not be compared directly because of the disparity in the controlling variables; strain and stress excursions

(Continues)

DD FORM 1 JAN 73 1473 EDITION OF 1 NOV 65 IS OBSOLETE
S/N 0102-014-6601

SECURITY CLASSIFICATION OF THIS PAGE (When Data Entered)

20. ABSTRACT (Continued)

respectively. It is found that both kinds of data form a consistent set if the total stress excursion is used as a basis of comparison, except for cases of overly high notch loading. The earlier strain-controlled results were modeled by a cumulative cyclic creep strain criterion for crack initiation. This criterion appears to embrace also the notch stress results, thus providing a promising means for extrapolating fatigue data.

CONTENTS

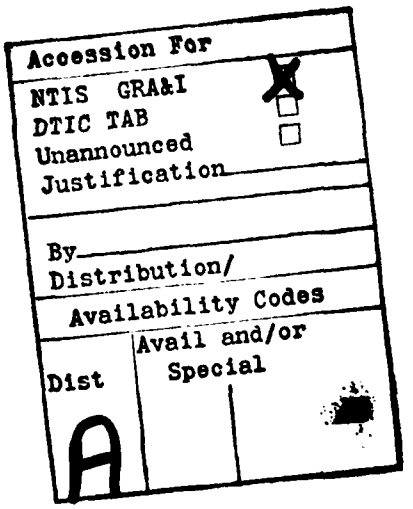

COMPARISON OF NOTCH-STRESS WITH STRAIN-CONTROLLED LOW CYCLE FATIGUE OF ALPHA-BETA TITANIUM ALLOYS

INTRODUCTION

This report is to document a measure of progress in an NRL program seeking improved fatigue resistance of titanium alloys for Naval jet engine parts. That large improvements in crack propagation resistance are possible has been demonstrated by Yoder et al. [1], who found increasing grain size to be beneficial. Since increased grain size tends to reduce crack initiation resistance, present authors are collaborating in a program to assess its effect, as well as that of oxygen content, on low cycle fatigue (LCF) crack initiation. To this end, Krafft has conducted tests on strain-controlled LCF, covering the range of endurance up to 10^3 cycles [2]. The long cycle period of the mechanical testing machine which was used precluded data in the 10^3 to 10^6 cycle range. To cover this, Yoder et al. have tested the same materials in notched tensile specimens under load control, using high speed electro-hydraulic servo type machines [3]. The object of this report is to display both sets of data together and to suggest a basis for their intercomparison.

MATERIALS AND TESTS

The alloys used are all of the Ti-6Al-4V system. Four 25.4 mm (1 in.) plates had been purchased with differing levels of interstitial oxygen. Specimens from each of the four plates were provided a grain coarsening anneal at temperatures above the beta transus. In addition, the highest-oxygen material was tested in its as-received condition as well as after a recrystallization anneal, both relatively fine grained. Repeated from the earlier reports, chemical analyses and heat treatment schedules and various mechanical properties are shown in Tables I, II and III respectively.

The material tested, specimens and manner of fatigue testing were described in the earlier reports. Briefly here, the strain controlled tests were performed in a screw-driven Instron machine, using small threaded "dog-bone" shaped tension-compression specimens, aligned in a subpress. Uniform head speed between strain-limiting stops provided a roughly triangular loading-wave form, of period about 40 seconds per cycle. Crack initiation was associated with changes in amplitude and form of the cyclic stress-strain curve.

For the tests of higher cyclic life, an MTS electro-hydraulic servo machine was employed, using load control and a sinusoidal loading wave form. For the earlier tests on the 0.020% oxygen material a loading frequency of 1 Hz was applied. Later with availability of a high speed machine, 20 Hz was applied to the three alloys of lower oxygen content. Specimens were of the

Manuscript submitted October 20, 1981.

1T WOL compact type with a half-height to width ratio of 0.486, as described by Saxena and Hudak [4]. These were notched with a 2.4 mm (3/32 in) slot to a relative depth of a/W=0.45, and bottomed with a finely honed end radius of 1.59 mm (.0625 in). Difficulty experienced in machining a suitable notch in specimens

Table I — Chemical Analyses

Alloy	Content (wt-%)								
	O	Al	Mo	V	Fe	N	C	H	Al*
Ti-6-4	0.06	6.0	—	4.1	0.05	0.008	0.023	0.0050	7.0
Ti-6-4	0.11	6.1	—	4.0	0.18	0.009	0.02	0.0069	7.6
Ti-6-4	0.18	6.6	—	4.4	0.20	0.014	0.02	0.0058	8.9
Ti-6-4	0.20	6.7	—	4.3	0.10	0.011	0.03	0.0060	9.2

Note: Al* is the aluminum equivalent

$$Al^* = Al + \frac{Sn}{3} + \frac{Zr}{3} + 10\,(O + C + 2N).$$

Table II — Heat Treatments for Ti-6Al-4V

Heat Treatment Type	Specification*
MA	788°C, 1 h /AC (as received)
RA	954°C, 4 h/HC @ 180°C/h to 760°C/AC @ 370°C/h to 482°C/AC
BA	1038°C, 0.5 h/HC to RT + 732°C, 2 h/AC

*Anneals performed in vacuum furnace; h = hour, WQ = water quench, FC = furnace cool, HC = cooled in He @ approx. air cooling rate , AC=air cool.

Table III — Mechanical Properties

Alloy		Heat Treatment		Orientation	0.2% Yield Strength σ_y (MPa)	Tensile Strength σ_{uts} (MPa)	Young's Modulus E (GPa)	Reduction in Area (%)	Elongation* (%)	Effective Grain Size $\bar{l}$ (μm)	$\frac{N_i}{L}$ (cycles)	SDF $\frac{\Delta\sigma}{\sigma_T}$
	Wt-% Oxygen	No	Type									
Ti-6-4	0.20		MA	T	1007	1034	130	29	14	5	6.0	2.18
Ti-6-4	0.20		RA	T	931	1007	130	26	15	9	7.0	2.19
Ti-6-4	0.20		BA	T	869	958	117	16	11	24	2.9	2.08
Ti-6-4	0.18		BA	T	818	906	120	13	8	38	3.4	2.08
Ti-6-4	0.11		BA	T	772	869	118	19	10	28	4.4	2.09
Ti-6-4	0.06		BA	T	740	818	115	34	10	17	8.0	2.07

at full 25 mm (one inch) thickness was lessened by parting the plate to provide a specimen thickness of 10 mm (0.4 in). Crack initiation and early growth was monitored visually with a travelling microscope. Notch stress was calculated using an elastic stress concentration factor for this configuration [5], resulting in a maximum notch stress of 64 psi per pound of applied load whereas, by virtue of its small 4.32 mm (0.170 in.) diameter, the tensile coupon developed a uniform stress of 44 psi per pound of axial load.

The compact tension specimens were loaded only in tension, unloading to 10% of maximum load, R = 0.1. This contrasts with the strain controlled cycling in which tensile straining is restored by plastic compression for an effective stress ratio R = -1. The direction of tensile stressing was the same in both, i.e., the long transverse direction.

DISPLAY OF BOTH DATA SETS

Differences in the manner of normalizing endurance values precludes direct comparison of the usual LCF data plots of these two test methods. Tension-compression LCF data is normally referred to plastic or total strain excursion, whereas notch fatigue data is associated with the notch-stress excursion. Since a measure of stress excursion is also available in the strain controlled test, it can be compared with the notch-stress excursion. Leis, et al [6] find close correspondence between smooth-specimen and notch-root fatigue endurance when the strain excursion in each is used as a basis of comparsion. Since uniaxial cyclic stress- and strain-excursion are uniquely related, correspondence with the stress excursion might be expected in regions of small plastic flow, where the elastic stress concentration factor is applicable. Thus in the data display, Figure 1, maximum or total tensile stress excursion in both kinds of tests is used as the basis of comparsion. For the strain controlled LCF, the maximum tensile stress excursion reached in the early cycles of fatigue, as measured on each test record and corrected to true stress, is plotted for each endurance value. For the notch--stress controlled LCF, the calculated (maximum) notch stress excursion is plotted. It does appear, Figure 1, that the combined data sets could represent a continuous trend, except for the notch tests at highest load levels. Exceptional endurance here could result from the plastic flow amelioration of the elastic stress concentration factor. As discussed later, the lines drawn through the data derive from the cyclic stress-strain curve of each material.

COMPARSION OF BOTH DATA SETS

The basis of comparsion used here is a cumulative tensile creep damage criterion resulting from the earlier strain controlled LCF study [2]. Here it was noticed that some of the titanium alloy/conditions exhibited markedly superior endurance. Coffin-Manson type plots of plastic strain excursion

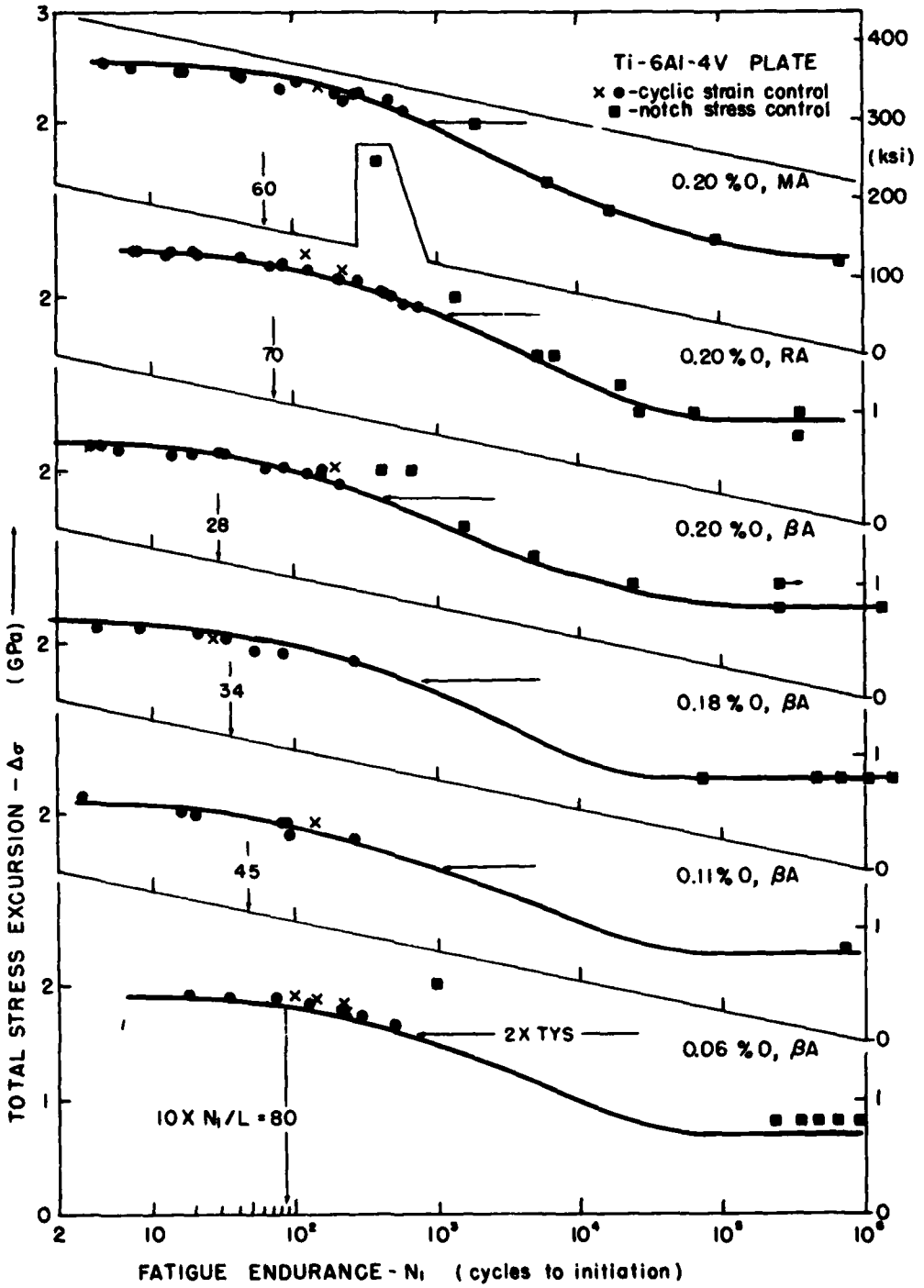

Fig. 1 — Fatigue crack initiation life relative to the total stress excursion, for both strain and stress controlled tests show consistency. The connecting curves are transient-creep-based life factor values from Fig. 3.

vs. endurance showed a bowing upward and to the right of the usual straight-line trend in logarithmic coordinates. It was noticed of the better performers that the shape of the cyclic hysteresis loops exhibited a characteristic evolution with cycling. Cyclic softening in the early part of a given cyclic excursion appeared to be restored by increased strain hardening in the latter part, resulting in an "inversion" in strain hardening rate. It was thought that the enhanced terminal strain hardening rate might increase endurance by reducing the amount of stress-relaxation-induced creep strain during the tension hold of each cycle. Tensile creep is known, after Halford et al. [7], to be the most damaging type of cyclic straining, from strain range partitioning analysis. In developing this hypothesis, a damage factor proportional to the cyclic creep per cycle, or its inverse as an LCF life factor L, was found to correlate nicely with the trends in crack initiation life of the various materials.

From this work, the stress-relaxation-induced creep strain, $-\Delta\varepsilon_c$ is approximately

$$\Delta\varepsilon_c = m \ln \left(1 + t_H / t_L\right) / \left(\Theta_p/\sigma_T - 1\right) \qquad (1)$$

where m is the stress relaxation exponent, t_L and t_H are loading and hold times of the straining (loading) cycle, Θ_p and σ_T are true values of the *tensile plastic strain hardening* rate and of the stress at the tensile extreme of the cyclic stress strain curve. The criterion for crack initiation is that the summation of creep strain (per cycle) reaches a critical level, ε_c, a constant of the material, independent of the cyclic strain range. In cases of a *non-evolving*, stable form of the cyclic stress strain curve, the tensile creep strain in each cycle is constant, due the stability of Θ_p and σ_T. In this case

$$N_i = \varepsilon_c / \Delta\varepsilon_c \sim \left(\Theta_p / \sigma_T - 1\right) \equiv L \qquad (2)$$

where N_i is the number of cycles to crack initiation and L, called the LCF life factor, is a function (only) of the form of the cyclic stress strain curve, as illustrated in Figure 2. In Ref. [2], a slightly different value of the coefficient ($L = \Theta_p/\sigma_T - \sqrt{3}/2$) was used. The unit value is used here because it is simpler and has no significant effect on the results. With the unit-value coefficient, L is simply the stress-relative plastic strain hardening rate of the material. In cases where the curve form "evolves" with cycling, an average value of L is found by summing its reciprocal, as a cumulative damage index, over the cyclic life. In these titanium alloys, the inversion/shift in Θ_p values with cycling appears to saturate at a constant level of a value which has little effect upon the L value in the higher cyclic life (high Θ_p) range. This fact is useful in that it allows an LCF life factor curve to be obtained by scaling a full, early cyclic, stress strain curve. Results of such scaling and calculation are shown in Fig. 3. Here values of L are measured out to the proportional limit, which should correspond to the endurance limit.

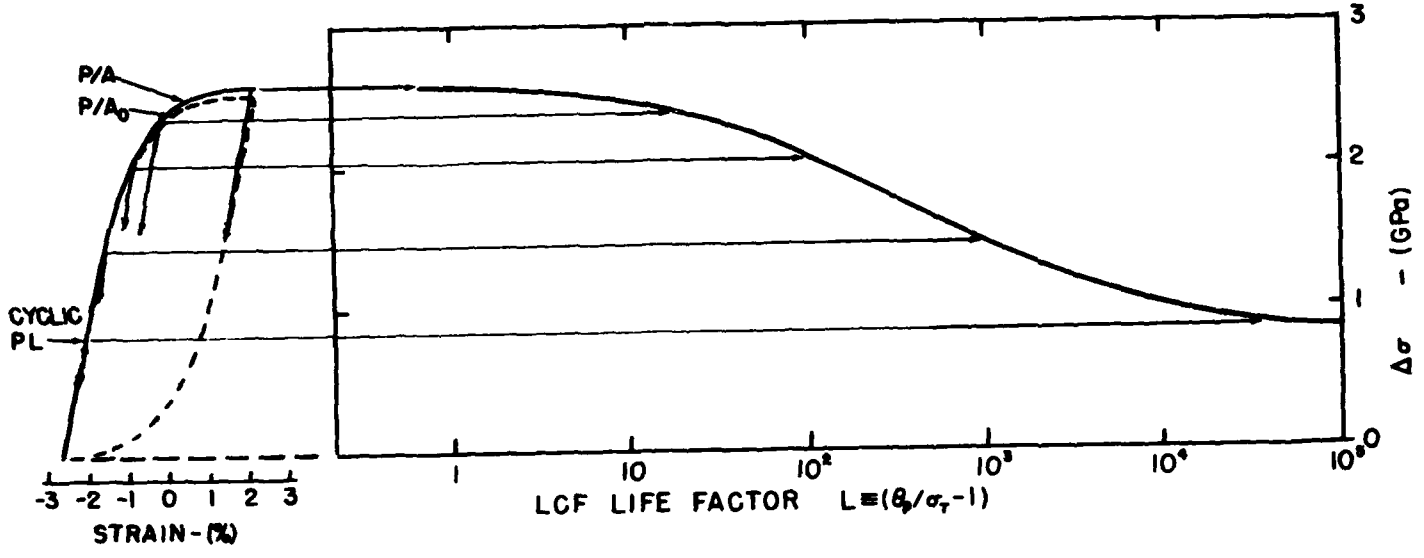

Fig. 2 — Development of LCF life factor (L) from the cyclic stress-strain curve

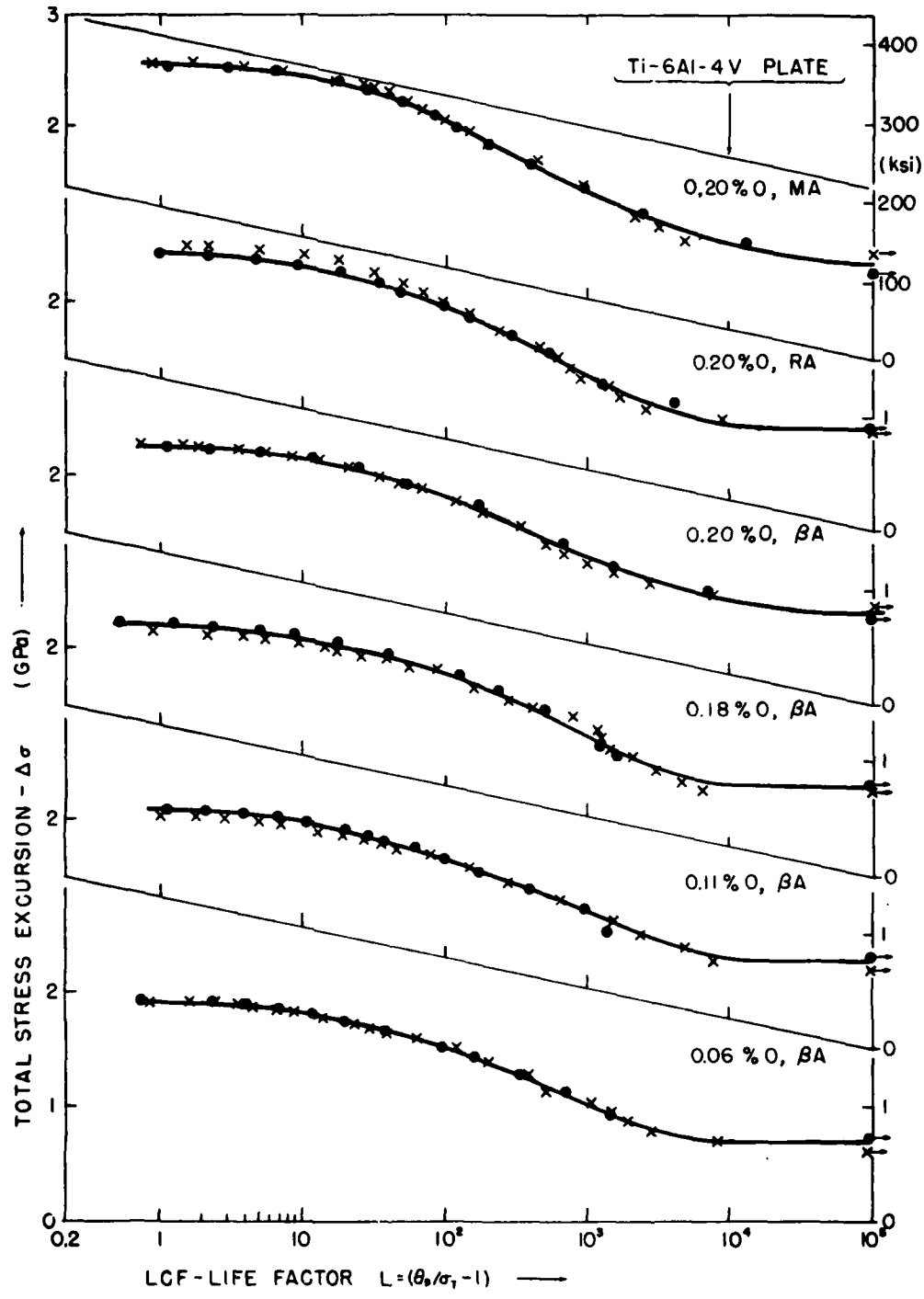

Fig. 3 — LCF life factor values, derived from full cyclic stress strain curves, are plotted on the stress scale of Fig. 1 for the various materials/conditions

Two sets of $\Delta\sigma_{max}$ vs. L data are shown. The one marked by x symbols is from stress-strain curves measured for earlier crack propagation modeling [8]. For best precision these were run at a slow machine head speed, 0.02 in/min. The second curve, marked by solid circles, is from measurements of a cyclic envelope during the fatigue test at 10X this speed, 0.2 in/min. Unfortunately, it was necessary to heat-treat additional material for the LCF test program. As a consequence, all L-value determinations at the higher strain rate are also of the second heat treatment batch. We believe the different batches of heat treatment had no signficiant effect on these results. The curves drawn through each of the $\Delta\sigma_{max}$ vs. L data sets favor the higher strain rate set, as more nearly approaching the loading frequencies of the notch-stress controlled fatigue tests.

It should be noted that the tensile stress σ_T which was used in Eq. 2 to calculate L-values reflects the strength differential effect in each alloy. The factor used, shown in Table III as SDF, is the divisor of the total stress excursion which yields the tensile portion for each test. For present comparisons, the total stress excursion is measured from the extreme compressive toe of the cyclic curve as illustrated in Figure 2.

Referring back to the endurance data, the curves shown in Fig. 1 are laid on directly from Fig. 3. The total stress excursion scales are, of course, the same. The matching of L to N_i scales is at the same ratios of N_i/L as found from the earlier strain-controlled data modeling. This assumption neglects differences between the cyclic wave forms and frequencies of the two tests, thought to be relatively minor ones for the purpose of establishing a basis of comparison.

Regarding a correspondence of between L and N_i, the three conditions of highest (0.20%) oxygen are most definitive, as most of the notch stress data was collected on these. In the range of high endurance, the prediction fits rather nicely. However at endurance levels below 10^3 cycles, the tolerance for notch-stress fatigue loading rises markedly. It is thought that this rise may reflect the reduction in the stress concentration factor [5], and that this is more dominant than the corresponding rise in the strain concentration factor. The effect of cyclic loading on the stress concentration factor is a further uncertainty. Arrows drawn at twice the tensile yield strength level in each plot roughly indicate the onset of this transition.

CONCLUSIONS

From this comparison and modeling of both strain and notch stress controlled LCF data on Ti-6Al-4V of varied oxygen content and grain size it is concluded that:

(1) The data sets form a consistent trend pattern when cycles to initiation are compared on a basis of total stress excursion.

(2) Referenced in this way, values of the stress-relative

cyclic plastic strain hardening rate, plotted vs. total stress excursion, nicely interconnect the data sets, hence provide a promising correlation basis.

(3) Departures from these trends for notch stress excursion levels greater than twice the yield strength could be due to the effect of plastic flow on the elastic stress concentration factor.

REFERENCES

1. G.R. Yoder, L.A. Cooley and T.W. Crooker, "50 Fold Difference in Region II Fatigue Crack Propagation Resistance of Titanium Alloys: A Grain Size Effect," J. Engineering Materials and Technology, 101, 86-89, January 1979.

2. J.M. Krafft, "Effect of Stress-Strain Behavior on Low-Cycle Fatigue of α-β Titanium Alloys," Fatigue of Engineering Materials and Structures, forthcoming (see also NRL Memo Report 4406, November 1980).

3. G.R. Yoder, L.A. Cooley and T.W. Crooker, "A Comparison of Microstructural Effects on Fatigue-Crack Initiation and Propagation in Ti-6Al-4V," Structural Dynamics and Materials Conference (AIAA/ASME), New Orleans, LA, 10-12 May 1982 (see also forthcoming NRL Memorandum Report, 1981).

4. A. Saxena and S.J. Hudak, Jr., "Review and Extension of Compliance Information for Common Crack Growth Specimens," Int. J. Fracture, Vol. 14, pp. 453-468, October 1978.

5. W.K. Wilson, "Elastic Plastic Analysis of Blunt Notched CT Specimens and Applications," J. Pressure Vessel Technology, 96, 4, November 1974, pp. 293-298.

6. B.N. Leis, C.V.B. Gowda and T.H. Topper, "Cyclic Inelastic Deformation and the Fatigue Notch Factor," Cycle Stress Strain Behavior, ASTM STP 519, 1973, pp. 133-150.

7. G.R. Halford, M.H. Hirschberg and S.S. Manson, "Temperature Effects on the Strain Range Partitioning Approach for Creep Fatigue Analysis," Fatigue at Elevated Temperatures, ASTM STP 520, 1973, pp. 658-669.

8. J.M. Krafft, "Case Studies of Fatigue Crack Growth Using an Improved Micro-Ligament Instability Model," NRL Memo Report 4161, January 1980.


DA
FILM